ORIGINAL PAPER

Geochemistry of thermal waters in the Changbaishan volcanic geothermal system, Northeast China—implications for vapor-liquid separation controls on geothermal fluid composition

Rongsheng Zhao[1] · Jian Yi[2]

Abstract

This work studied the geochemistry of the Changbaishan volcanic two-phase geothermal system in northeastern China. The fluid geochemistry and existence of hot fumaroles (with temperatures greater than 100 °C) and sinters imply the occurrence of vapor-liquid separation at depth, and the B/Cl and Na/Cl ratios imply a second vapor-liquid separation process. The extremely low B/Cl ratios and Hg concentrations below the detection limit in the sampled well water indicate that the process in the deep reservoir has approached the late stage. Statistical analysis shows that Na, Mg, Li, Sr, B, Fe, Zn, HCO_3^-, and Cl^- are the characteristic elemental constituents of the geothermal system, and the type A elements (Fe, Zn, Li, B, Sr, and Mg) are mainly controlled by the vapor-liquid separation in the reservoir. As the water rises, the concentrations of the type A elements are controlled by fluid-rock interactions and the dilution process. In contrast, the type B elements (Cl^-, Na, and HCO_3^-) are mainly controlled by the vapor-liquid separation accompanying the input of magmatic volatiles. The Na/Li geothermometer indicates that the first vapor-liquid separation process occurs at 297 °C, and the Na–K–Ca geothermometer indicates that the second vapor-liquid separation process occurs at 328 °C. With the isotopic fractionation characteristics at different temperatures, our reassessment of the δ^2H and $\delta^{18}O$ data implies that the water in the hot springs originates from different mixtures of precipitation and steam-heated water that has experienced multiple separation processes. In addition, a large flux of CO_2 has lowered the $\delta^{18}O$ values, causing a shift to the left of the local meteoric water line.

Keywords Volcanic geothermal system · Fluid geochemistry · Vapor-liquid separation · Magmatic volatiles · Fluid-rock interaction

Introduction

The phase separation process is a common phenomenon in geothermal systems in volcanic areas (Arnórsson et al. 2007; Guo et al. 2020; Ingebritsen and Sorey 1988; White et al.

✉ Jian Yi
187082873@qq.com

Rongsheng Zhao
15246007162@163.com

[1] College of Biological and Agricultural Engineering, Jilin University, 5988, Renming Road, 130022 Changchun, People's Republic of China

[2] Earth Science College, Jilin University, 2199 Jianshe Street, 130061 Changchun, People's Republic of China

1971). Depressurization or "excess heat" input can cause this process, which can modify the composition of water that had previously been controlled by temperature-dependent fluid-rock equilibrium (Henley and Hughes 2000; Janik and Mclaren 2010; Kaasalainen and Stefánsson 2012; Kaasalainen et al. 2015; Nuccio et al. 1999; Scot et al. 2014; Stefánsson et al. 2017). After separation occurs in the reservoir, nonvolatile elements, such as Cl and Na, remain in the liquid, while volatiles, such as C, S and B, ascend with the hot vapor and condense near the surface (Giggenbach 1992; Leeman et al. 2005; Stefánsson et al. 2017; Zhao et al. 2019). In addition, depressurization may lead to the partitioning of some metal elements, such as Hg and Sb, between the vapor and liquid phases (Kaasalainen and Stefánsson 2012), although the metal concentrations in the low-density vapor formed by the low-pressure boiling of geothermal fluids are generally considered negligible (Heinrich 2007). Alkaline waters are considered to represent boiled

water, and steam-heated acid-sulfate waters are considered to form by the mixing of steam with surface water or steam condensation. Thus, according to their major chemical compositions and formation mechanisms, surface geothermal waters can be categorized as alkaline waters, steam-heated acidic waters, CO_2 waters, and mixed waters (Allen and Day 1927; Arnórsson et al. 2007; Fournier 1989; Giggenbach and Stewart 1982; White 1957). However, due to fluid-rock interactions, in many cases, steam-heated sulfate waters are neutral and not acidic (Arnórsson et al. 2007; White et al. 1971). The temperature, chemical evolution, and flow path of geothermal fluids are essential factors of a reservoir for assessing the potential for power generation and sustainable use of geothermal resources (Heřmanská et al. 2020; Yan 2016; Kaasalainen and Stefánsson 2012). Nevertheless, the study of this geothermal system is mainly focus on vapor-liquid separation process (Zhao et al. 2019), chemical evolution (Rahayudin et al. 2020), numerical (Scott et al. 2017) and experiment (Heřmanská et al. 2020) simulation, and the knowledge of the trace element composition characteristics during vapor-separation process in such geothermal systems remains limited.

Changbaishan (or Mt. Baekdu; CBS), a Cenozoic active volcano in Jilin Province, Northeast China, is associated with many well-known springs, which are recharged mainly by precipitation (Lin et al. 1999; Yan 2016; Zhao et al. 2019). The chemical and isotopic characteristics (δ^2H, $\delta^{18}O$, $\delta^{13}C$ and tritium (T) values) of the CBS geothermal system (CGS) have been studied in detail (Lin et al. 1999; Shangguan et al. 1996; Shangguan et al. 1997; Yan 2016; Zhang and Li 2006), and a genetic model based on a liquid-dominated system has been established (Yan 2016; Yan et al. 2016). However, this model is hindered by the fact that it cannot precisely explain the low $\delta^{18}O$ and δD values in the thermal water and the low flux of producing wells. A recent survey using B isotopes and gas data found that the CGS is a two-phase system (Zhao et al. 2019); due to boiling processes, approximately 75~87.5% of the water becomes vapor in the deep reservoir. However, whether the liquid-dominated or two-phase geothermal system model is correct, in these models, the geochemical characteristics, especially the trace element compositions of the geothermal fluids, have received less attention than the associated geologic structures, estimation of resource reserves, gases, and water origins (Chen and Wang 2012; Guo et al. 1996; Huang et al. 2020; Jiang and Chen 2015; Lin et al. 1999; Liu et al. 2015; Yan 2016; Wei et al. 2013), and this gap in the research has hindered reasonable geothermal source development.

Therefore, based on the vapor-liquid separation process, the present study aims to investigate (1) the fluid geothermal characteristics, (2) the factors controlling the fluid compositions, and (3) the formation mechanism of low $\delta^{18}O$ and δD values in the CGS. We believe that the results of this study will improve the understanding of the two-phase geothermal system's element enrichment mechanism and promote the

further optimization of the exploitation and utilization of geothermal resources.

Geological setting

CBS is located between Northeast China and the Korean Peninsula, and its formation is related to Cenozoic volcanism (Chen et al. 2007; Liu et al. 1997; Zhao et al. 2019). The eruption history has been well reconstructed by K-Ar and ^{14}C dating (Liu et al. 2015; Wang et al. 2003), and minor eruptions have occurred as recently as 1903 (Xu et al. 1993). The exposed rocks around the crater area are basaltic to trachytic/rhyolitic (Shi et al. 2005), while Precambrian metamorphic rocks, Phanerozoic carbonate rocks, and Mesozoic clastic rocks can be found in the peripheral area (Fig. 1(b, c)). The basement is composed of Paleozoic to Mesozoic sedimentary rocks (clastic and carbonate rocks) with local Archean and Mesozoic granitic intrusions and minor Precambrian metamorphic rocks (Yi et al. 2016), which have been drilled in the CR2 well, ~ 45 km west of the Tianchi crater. The area is affected by three fault systems: NE-SW compressional-shear faults, NW-SE transtensional faults, and N-S extensional faults. The NE-SW-trending Yalujiang lithospheric fault formed by collision of the Longgang area with the Helong area (Fig. 1(a)) controls the regional geologic structure. In addition to the major magmatic intrusion below the Tianchi crater area (at a depth of 7–17 km; Qiu et al. 2014), many minor ascending submantle plumes exist along the periphery of the region and form the basic heat sources of the CGS (Zhao et al. 2009, 2019).

The topography is composed of a series of northeast-trending mountain chains and intermontane basins. The terrain is high in the southeast and low in the northwest, with a gradient of approximately 10°. The Tianchi crater of CBS is the source of many large rivers in Jilin Province (Zhu et al. 1981), such as the Songhuajiang River, and features many famous mineral water factories. The study area features a continental monsoonal climate, and the winter lasts from September to April of the following year, with a mean temperature of approximately − 7.3 °C. The annual average amounts of precipitation and evaporation at the Changbai Mountain Tianchi weather station are 1332.6 mm and 1180 mm, respectively (Geological environment monitoring station of Jilin Province 2004).

Sampling and analysis

Six hot springs, two cold springs, two wells, and two crater water samples from the CBS area were collected in July 2018 (see sampling locations in Fig. 1). Sampling of water samples was carried out by following the guidelines set by
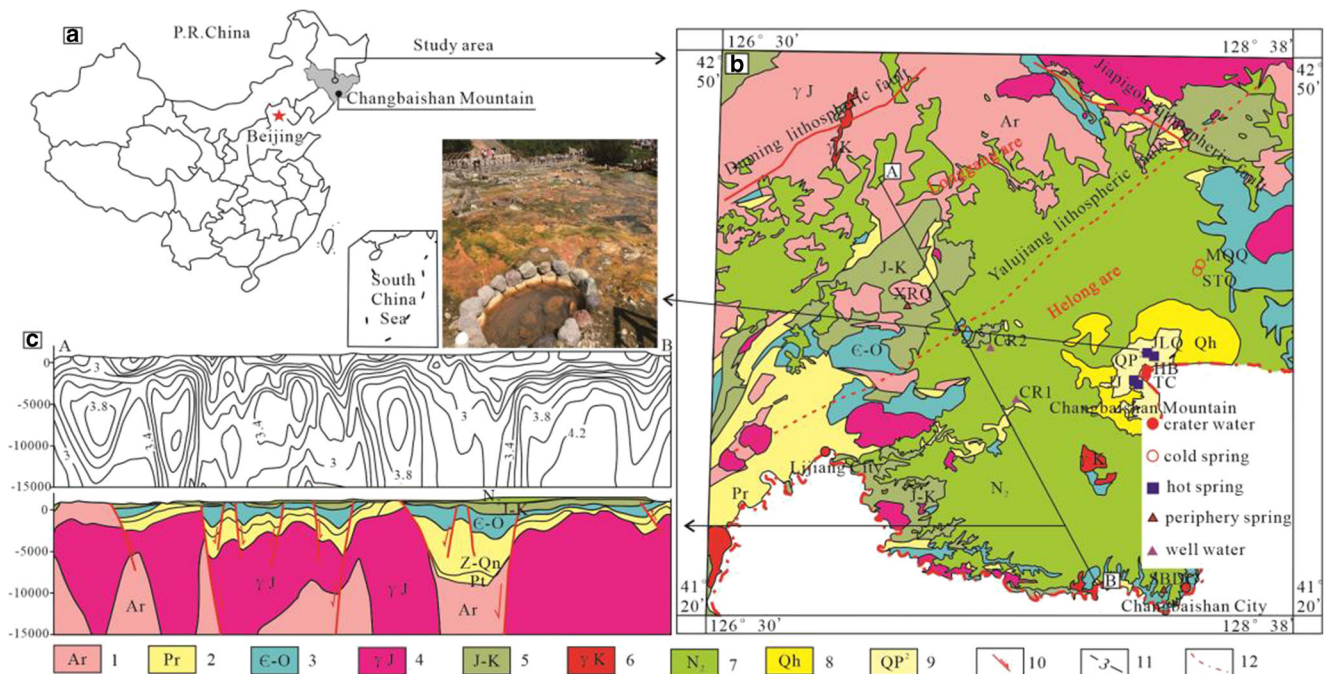
Fig. 1 (a) Location of the CGS; (b) modified from the 1:250000 geological map; and (c) is the MT sounding observation profile and its geological interpretation. (1) Archean granite, (2) Proterozoic metamorphic rock, (3) Cambrian and Ordovician clastic and limestone rocks, (4) Jurassic granite, (5) Mesozoic clastic rock, (6) Cretaceous granite, (7) Neogene basalt, (8) Holocene pyroclastic rock, (9) Holocene trachyte, (10) Fault, (11) Contour line, and (12) Boundary line. (modified from Zhao et al. 2019)

Ármannsson and Ólafsson (2006). The in situ temperature and pH were measured using Orion 4-Star meter. Water samples were filtered through a 0.45-μm filter (cellulose acetate) into precleaned high-density polyethylene bottles. Before sampling, the filtering device was flushed with 250 ml of sample. Samples for trace metal analysis were acidified to pH < 2 with ultra-pure HNO_3, while those for anion analysis were left unacidified.

Anions (Cl^-, SO_4^{2-}) were determined using ion chromatography (IC, Dionex ICS 2100), and major cations (Na^+, K^+, Ca^{2+}, and Mg^{2+}) were determined by atomic absorption spectrophotometry (AAS, Perkin-Elmer Pinaacle 900F). SiO_2 contents were analyzed by a portable photometer (Hanna HI96705), and HCO_3^-/CO_3^{2-} contents were analyzed by Gran titration in the laboratory on the day of sampling. The concentrations of selected trace elements (Li, Cs, Rb, Sr, Ba, B, As, Al, V, Cr, Mn, Fe, Ni, Cu, Zn, and Mo) were analyzed using high-resolution inductively coupled plasma mass spectrometry (HR-ICP-MS). The geochemistry was analyzed at the Jilin University Test Center, China, with a precision for all analyses of better than ± 5%. Quality of analytical was ensured by using check standards, commercial standard solutions, reagent blanks, recovery of spike, and replicate analysis. The percentage error for the charge imbalance calculated using PHREEQC program (Parkhurst and Appelo 1999) with phreeqc.dat database yielded a mean value of 2.98% with maximum and minimum values of 0.37 and 7.01%, respectively.

Results and discussion

Hydrochemistry

In the CBS geothermal field, the water samples are mostly nearly neutral fresh water, with the exception of the well water samples, which have a maximum total dissolved solids (TDS) value of 9736.2 ppm and belonged to the neutral saline water category (Table 1). HCO_3^- is the predominant anion of the samples (except the sample from XRQ, in which SO_4^{2-} is the predominant anion), Na^+ is the predominant cation, and the concentration of Mg^{2+} is generally low (Table 1, Fig. 2). According to the Schakerev classification, the water facies of the crater-area hot springs and the crater water samples are Na-HCO_3, those of the peripheral springs are Na-HCO_3-Cl (site SBDG) and Na-HCO_3-SO_4 (site XRQ), that of the well waters is Na-Ca-HCO_3-Cl, and that of the cold springs is Na-Ca-HCO_3 (Fig. 2). The two crater water samples are from the same crater (CBS Tianchi crater), but the HB sample is from a location with a relatively higher gas concentration than that of the TC sample. The concentrations of Na^+, HCO_3^-, Cl^-, SiO_2, Li, Sr, B, Mn, and Ni of the HB water sample are higher than those of the TC sample, especially the concentration of B, but the pH, Rb, Fe, and Zn values are lower in the HB sample than in the TC sample (Tables 1 and 2).

In the comparison of the crater water with the cold springs water, which is entirely recharged by precipitation (Yan 2016), the former features higher element concentrations,

Table 1 General hydrochemical properties of the thermal water collected from the Changbaishan area

Sample	Description	Temp (°C)	pH	K ppm	Na	Mg	Ca	HCO_3^-	SO_4^{2-}	Cl^-	SiO_2	TDS	pCO_2 atm	$(HCO_3^- + SO_4^{2-})/(Ca^{2+} + Mg^{2+})$
TC	Crater water	3.0	7.2	5.9	53.3	0.7	10.9	126.0	4.5	26.1	35.6	150.0	0.0071	11.25
HB	Crater water	3.0	6.8	6.1	65.9	0.9	9.8	174.0	4.5	18.5	45.2	212.7	0.0206	16.68
MQQ	Cold spring	5.6	6.5	2.7	7.0	1.9	4.6	29.7	7.2	1.4	34.3	70.3	0.0056	5.68
STQ	Cold spring	5.7	6.6	2.9	10.0	2.3	4.7	39.6	5.6	1.6	44.1	70.5	0.0065	6.46
JJ-1	Hot spring	59.0	6.6	30.6	363.0	13.3	33.0	966.9	21.2	98.2	238.9	232.3	0.1503	21.34
JJ-2	Hot spring	53.5	7.1	21.2	304.0	11.3	26.0	827.5	21.2	53.5	203.6	157.2	0.0536	22.75
JLQ-1	Hot spring	82.0	7.3	20.0	378.0	1.9	28.5	898.6	2.3	69.6	189.4	282.1	0.0385	29.63
JLQ-2	Hot spring	73.0	7.2	20.5	375.0	2.0	17.8	951.9	1.3	38.9	193.1	264.1	0.0502	48.14
XRQ	Hot spring	53.5	7.3	9.5	404.0	2.1	31.0	414.3	500.6	138.8	71.8	164.0	0.0174	27.64
SBDG	Hot spring	35.5	7.3	10.1	335.0	10.1	34.9	702.7	84.9	123.9	52.1	746.0	0.0301	1.16
CR1	Well	31.0	6.8	21.2	1467.0	245.9	434.0	3237.5	59.4	1907.2	68.1	7456.8	0.3295	11.04
CR2	Well	25.0	6.6	27.1	1986.0	281.0	492.5	3813.0	68.9	2632.0	64.3	9736.2	0.5375	5.02
p-level[a]	t-test	<0.05	>0.05	>0.05	<0.05	<0.05	>0.05	<0.0001	>0.05	<0.0001	>0.05	<0.0001	na	na

[a] In both Table 1 and Table 2, the t-test was conducted between the hot spring and well water samples; *na* not analyzed

except for Mg^{2+}. The low ion concentration and TDS values of the hot spring water samples in both the crater area and periphery imply rapid circulation, although the T value indicates a longer time (ranging from below 3 TU to 25.8 TU; Lin et al. 1999; Yan 2016). Since most of the tritium produced by the atmospheric testing of thermonuclear bombs between 1951 and 1980 has been washed from the atmosphere and the T values in global precipitation are now close to natural levels, the T dating method has been replaced by methods based on chlorofluorocarbons (CFCs), SF_6 and other compounds (Santoni et al. 2016; Tan et al. 2014). The observed geochemistry implies that fluid-rock interaction is not the main factor controlling the element composition of the CBS-area thermal water, and this inference is supported by the poor correlations of TDS/temperature, Cl/temperature, Na/Cl, and TDS/Cl (Fig. 3(a–d)).

Fluid composition

Classification of water

To better understand the formation mechanisms of the water and the mechanisms controlling the fluid composition, Q-cluster analysis was applied to all water samples based on the element compositions. For elements below the limit of detection, we used a concentration value equivalent to half the limit of detection in the analysis (Fig. 4).

Based on the cluster results in Fig. 4, the samples can be divided into three groups: Group 1 (cold water, i.e., both the crater and cold spring water), group 2 (low-Cl hot spring water), and group 3 (high-Cl well water). Based on previous research (Zhao et al. 2019), due to multiple vapor-liquid separation processes occurring at depth, the low-Cl thermal waters are related to steam-heated/condensate water, and the high-Cl thermal water are related to the residual water. The difference between the two crater waters may be due to the input of interaction between deep acidic magmatic volatiles and the host rock (Gao et al. 2006; Shangguan et al. 1996) and/or may be a result of mixing with steam condensation water. The Na/Cl ratio can be used to distinguish the two factors (Aggarwal et al. 2000). The input from magmatic volatiles may lead to a lower Na/Cl ratio because Cl is input as HCl^0. Furthermore, Na and Cl show similar behaviors during vapor-liquid separation, while B is more volatile (Ármansson et al. 1982). Hence, the lower Cl/B ratio (1.64) and slightly higher Na/Cl ratio (3.56) in the TC water sample than in other samples (with values of 53.67 and 3.31, respectively) indicate the input of steam from vapor-liquid separation. However, we cannot exclude the input of magmatic volatiles, as the B concentration is an order of magnitude higher in the crater samples than in the well water samples, and the gas shows an obvious deep origin (Gao et al. 2006; Shangguan et al. 1996). The geochemistry of the hot spring water samples also

Fig. 2 Compositions of all crater, cold spring, and hot spring water samples collected from the Changbaishan volcanic zone plotted on a Piper diagram
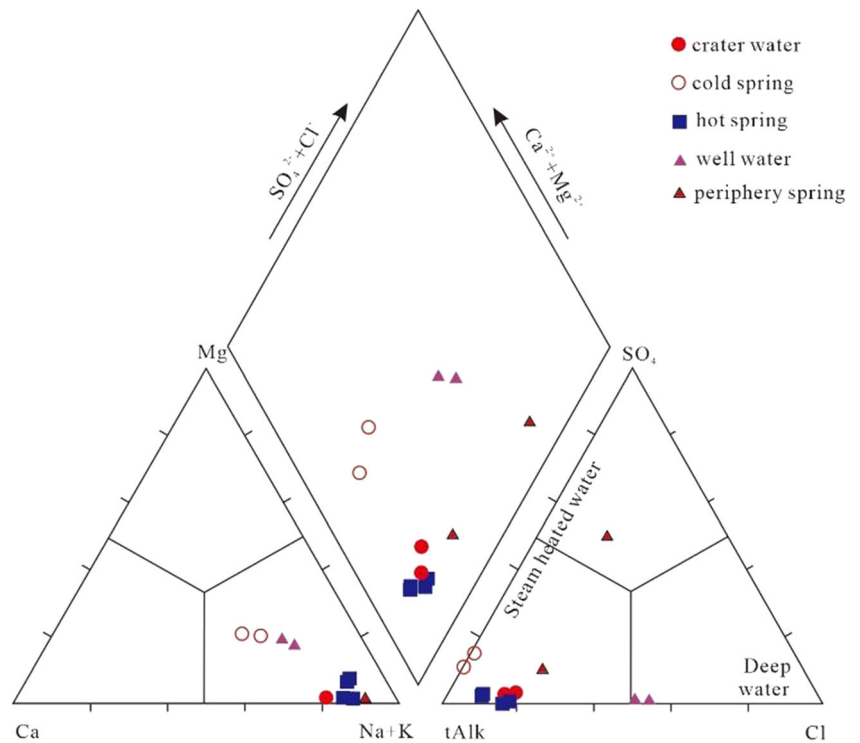
Table 2 Minor and major trace elements of water collected from the Changbaishan area

Sample	Li	Cs	Rb	Sr	Ba	B	As	Al
				ppb				
TC	98	3	48	18	4	300	–	40
HB	110	2	42	21	3	11300	–	–
MQQ	3	–	5	19	3	< 0.1	–	50
STQ	4	–	7	15	1	< 0.1	–	30
JJ-1	573	12	148	89	53	1500	20	70
JJ-2	479	13	112	112	16	900	10	20
JLQ-1	522	55	181	49	5	1700	30	–
JLQ-2	529	55	187	47	4	1600	30	40
XRQ	630	26	45	3110	29	900	–	20
SBDG	739	63	71	818	117	1000	–	40
CR1	3290	2	36	14100	20	150	–	60
CR2	3213	2	nd	78080	35	200	6	125
p-level	< 0.0001	> 0.05	> 0.05	< 0.05	> 0.05	< 0.05	> 0.05	> 0.05
Sample	V	Cr	Mn	Fe	Ni	Cu	Zn	Mo
				ppb				
TC	–	–	1	10	–	–	20	2
HB	–	–	27	–	6	–	–	2
MQQ	2	–	1	20	1	2	10	1
STQ	2	–	–	10	–	1	–	4
JJ-1	–	5	95	410	1	1	10	15
JJ-2	–	4	94	520	–	1	–	11
JLQ-1	–	4	22	510	4	1	–	3
JLQ-2	–	4	–	20	2	1	–	3
XRQ	–	1	11	50	–	2	–	19
SBDG	–	4	7	10	–	1	–	–
CR1	1	15	–	1610	2	1	63	1
CR2	–	–	9	1736	–	3	106	nd
p-level	> 0.05	> 0.05	> 0.05	> 0.05	> 0.05	> 0.05	< 0.05	> 0.05

"–" below detection limit; elements below the detection limit in all water samples were not listed
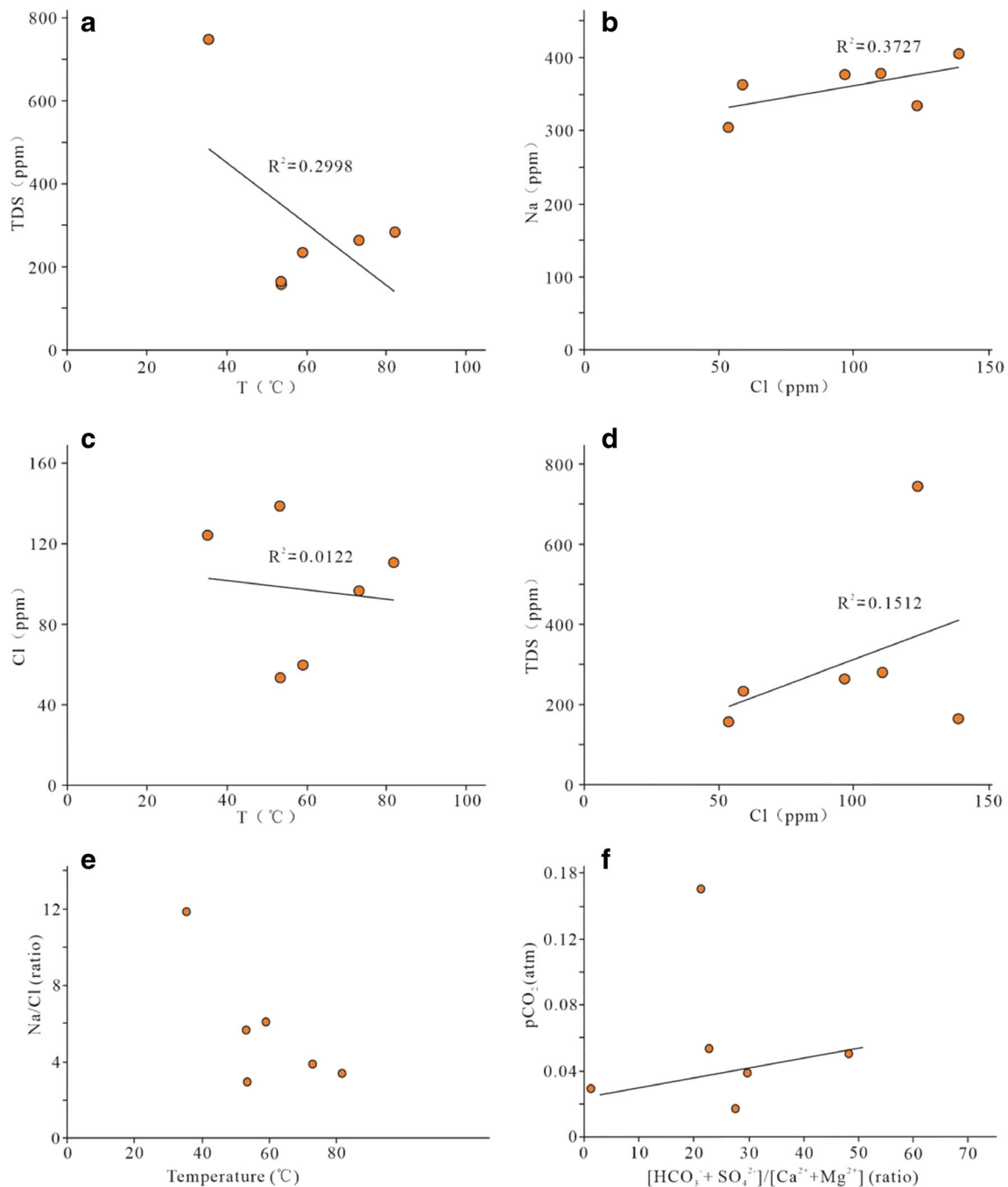
Fig. 3 Plots of TDS vs. temperature, Cl vs. temperature, Na vs. Cl, TDS vs. Cl, Na vs. Cl and pCO2 vs. $[HCO_3^- + SO_4^{2-}]/[Ca^{2+}+Mg^{2+}]$ for the hot spring water samples collected from the Changbaishan area

shows a different character. The springs in the crater area (JLQ and JJ) overlap with the springs in the periphery area (XRQ and SBDG) with a larger rescaled distance than the others, which may be due to differences in the vapor-liquid separation process, mixing with near-surface water or a different secondary reaction, such as fluid-rock interactions (Harun et al. 2020).

The Cl/B ratio of hydrothermal waters can be used to identify subsurface processes, such as water-rock interactions,
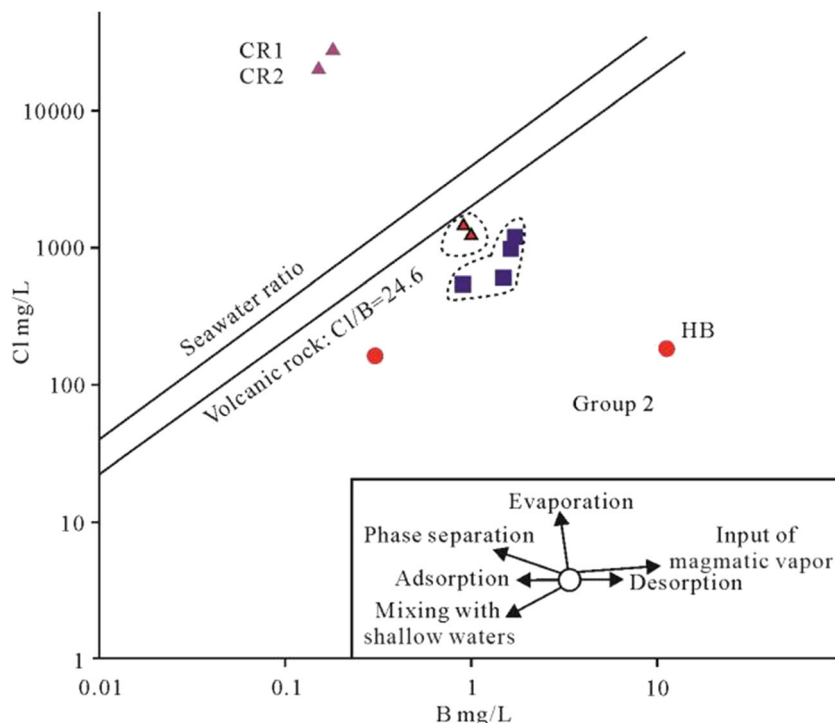
magma degassing and seawater involvement in a geothermal system (Arnórsson and Andrésdóttir 1995; Bernard et al. 2011; Purnomo and Pichler 2014; Valentio and Stanzione 2003). Similar to the division of hydrochemical characteristics, the three types of water samples can also be distinguished by their Cl/B ratios (Fig. 5). HCl is a nearly universal volcanic fumarole gas constituent that always exists at concentrations of 0.5 to 1 mil% of the total gas (Truesdell et al. 1989) and forms in high-temperature and low-pressure magmatic
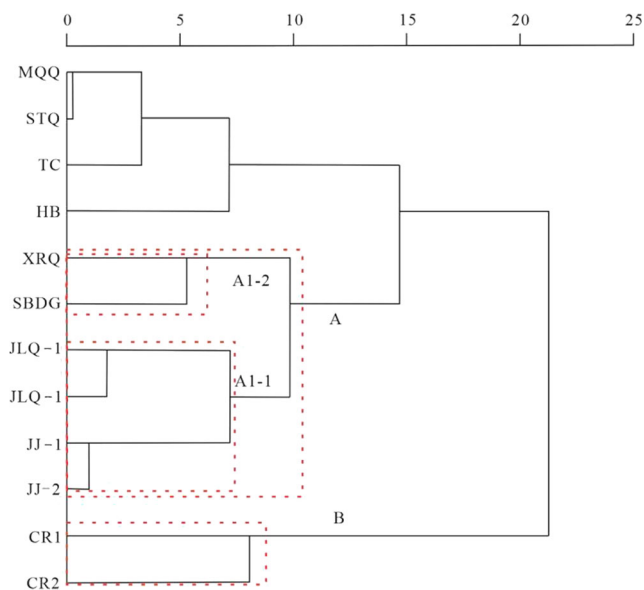
Fig. 4 Q-cluster of the thermal water from the Changbaishan volcanic zone

systems (temperatures higher than 160 °C; Truesdell et al. 1989). However, even when this value is added to the seawater, the high Cl/B ratios of the CR1 and CR2 thermal water samples (3939.75 and 453083, respectively) are not reached. The concentration of boron is especially low, and the B/Li ratio is anomalous, as B is always considered more volatile than Li during magma degassing (White 1957) and the concentration of Li in water is generally controlled by the surrounding rocks (Ellis and Mahon 1964; Vengosh et al. 1991).

Therefore, the unusually high Cl/B values of CR1 and CR2 result from the phase separation process. The steam-heated/condensate water samples (hot spring water) all have Cl/B ratios that exceed the highest Cl/B ratio of volcanic rocks, which implies that fluid-rock interaction is not the main mechanism controlling the hydrochemical composition of the water. Yan (2016) relates this high ratio to an evaporation process; however, the production of this value would require continuous evaporation in the surface environment, and the CBS area has a continental monsoonal climate, which is not an open environment. Therefore, this mechanism can be excluded. Even though the hot spring waters show a high degree of mixing with near-surface water, the maximum temperature can still approach 82 °C (near the boiling point of 90 °C). In addition, the Na/Cl ratio and temperature are not correlated (Fig. 3(e)); thus, we conclude that the hot spring waters have experienced a second vapor-liquid separation process due to the hot magmatic volatile input, as the gases collected from all hot spring areas show a mantle origin (Shangguan et al. 1997). To further understand the geochemical formation mechanism, we discuss the origin of the elements in the thermal waters (group 2 and group 3) below.

The main factors controlling the fluid composition

The geochemical patterns associated with different origins or processes always display regular combinations of element characteristics (Yu et al. 1990; Zhao et al. 2018). Therefore, R-model cluster analysis can be used to identify these

Fig. 5 The correlation between B and Cl. The diagram was modified from Zhao et al. (2019). The legend is the same as in previous figures

combinations based on the correlations among different elements (Guo and Wang 2012; Negri et al. 2018; Yu et al. 1990; Zhao et al. 2018).

Notably, the different types of elements (Na, Mg, HCO_3^-, Cl^-, Li, Sr, B, Fe, and Zn) in group 2 and group 3 show a uniform divide: type A includes Fe, Zn, Li, B, Sr, and Mg, while type B includes Cl^-, Na, and HCO_3^- (Fig. 6). This divide is also shown by the t-test analysis (Table 1, Table 2). The uniform classification of the two groups may indicate that they experienced similar processes in different reservoirs, although they have greatly different hydrochemical features. In the previous analysis of thermal water hydrochemistry, the following processes were inferred to control the compositional characteristics of the waters in the CBS area: (1) vapor-liquid separation, (2) input of magmatic volatiles, (3) fluid-rock interactions, and (4) mixing with near-surface water (precipitation). To further distinguish the impacts of these factors on the two types of elements, the relative concentrations of Li-Rb-Cs and Cl-Li-B were studied (Giggenbach 1991), as these elements have relatively low degrees of reactivity within geothermal systems (Giggenbach and Goguel 1989; Gurav et al. 2016).

The well water samples plot far from the rock dissolution lines and are obviously different from the hot spring and cold spring water samples (Fig. 7), which implies an origin from a different reservoir (e.g., Wragea et al. 2017). The concentrations of Li and Cl^- in the well water samples are an order of magnitude higher than those in the spring water samples. In contrast, the concentration of B in the well water samples is an order of magnitude higher than those in the spring water samples, and the Rb and Cs concentrations are also significantly lower in the well (Table 1, Table 2). The low Rb concentration may be due to the dissolution of illite at temperatures higher than 300 °C before mixing, while the low Cs concentration may be related to the dissolution of zeolites via the outflow process. However, the concentration of Li in the water samples is higher than the highest concentrations present in

igneous rocks (1.8 ppm, Ellis and Mahon 1967) and seawater (0.028 ppm), even after undergoing dilution, which implies that the well water has experienced a concentration process. Thus, the main control factor before fluid ascent was vapor-liquid separation that did not involve evaporation, as noted by the discussion of the B/Cl ratio. In this way, the high concentrations of the alkali earth metal Sr and the pH-dependent transition metals Fe and Zn in the well water can also be explained. Furthermore, Sr is abundant in marine sediment (Gurav et al. 2016), and there are no significant pH differences between the two thermal water groups. The Li, Rb, and Cs concentrations of the hot spring water samples are located mainly around the rock dissolution line in Fig. 7(a) and are different from those in Fig. 7(b), which shows the absorption of low B/Cl steam in a relatively old hydrothermal system. This difference indicates that the hot spring fluid composition is controlled by a vapor-liquid separation process. Therefore, the well water composition is related to the loss of steam, while the hot spring water composition is related to absorption. Additionally, the B/Cl ratio of the JJ thermal water is higher than those of other samples because the JJ site is close to a fracture from which steam rises, as verified by gas data (Shangguan et al. 1996; Zhang et al. 2015). Thus, we conclude that type A elements are mainly controlled by vapor-liquid separation in the reservoir, and when the water rises, the fluid composition is impacted by fluid-rock interactions and dilution.

As discussed before, the behaviors of Na and Cl differ between vapor-liquid separation and the input of magmatic volatiles: in the former process, these elements exhibit a poor correlation, while in the latter process, the Na/Cl ratio decreases (Aggarwal et al. 2000). There is a poor correlation between Na/Cl and temperature in the hot spring water samples from the CBS area (Fig. 3(e)), which indicates that the dominant process controlling the hydrochemistry is vapor-liquid separation. However, the gas collected from the hot spring area shows a high concentration of CO_2 (higher than
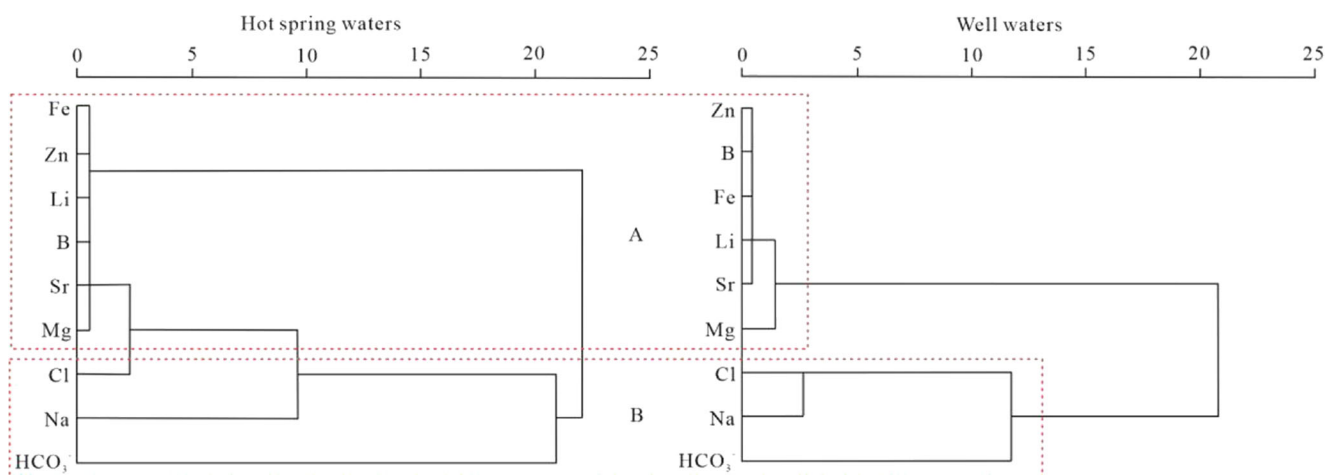
Fig. 6 R-model cluster analysis dendrogram for elements in hot spring and well water samples in the Changbaishan area
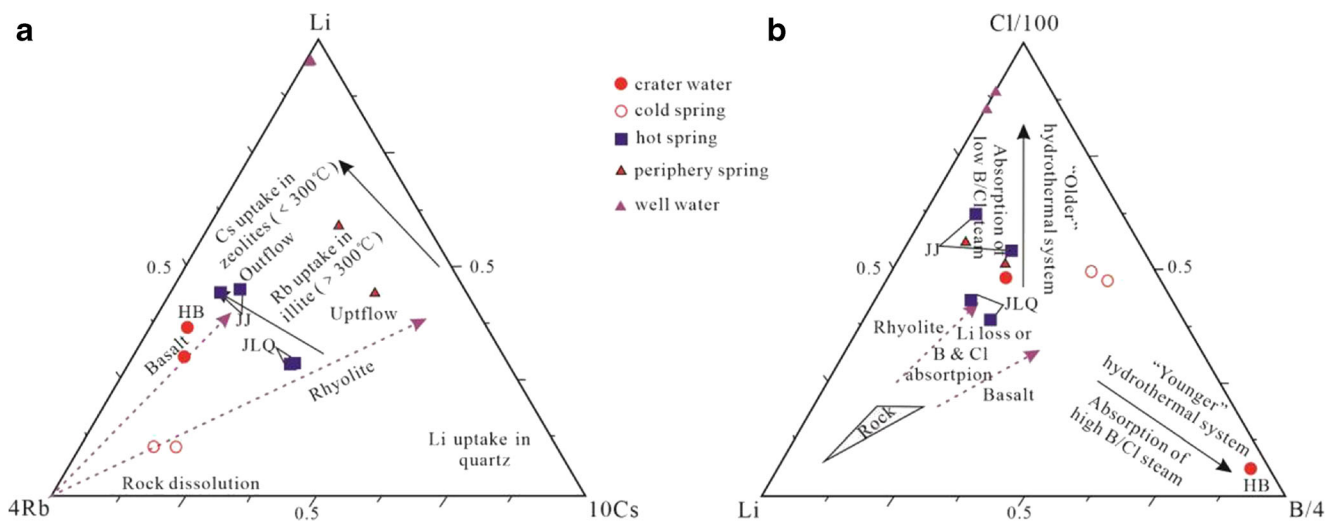
Fig. 7 Relative concentrations of Li-Rb-Cs and Cl-Li-B (µg/kg). Domains/processes are indicated by the text and arrows and were defined by Giggenbach (1991). The rock elements are from the average crustal rock composition reported by Gurav et al. (2016)

80%) with a δ^{13}C value ranging from -7.5 to $-4.2‰$, which indicates a mantle origin (Shangguan et al. 1997). The main anion of the thermal water in the CBS area is HCO_3^-. If the formation of the high HCO_3^- concentration is related to rock leaching (e.g., carbonate and anhydrite), the ratio of $[HCO_3^- + SO_4^{2-}]/[Ca^{2+}+Mg^{2+}]$ should be 1; in contrast, if the ratio is higher than 1 (Table 1), the HCO_3^- in the CBS area is derived, at least partially, from the interaction between waters with CO_2 gas (Karimi et al. 2017). In addition, the positive correlation between $[HCO_3^- + SO_4^{2-}]/[Ca^{2+}+Mg^{2+}]$ and carbon dioxide partial pressure (pCO_2), which can be calculated based on $lg(K^2/Mg)$ and $lg(K^2/Ca)$ (Giggenbach 1988), further confirms the influence of magmatic volatile inputs (Fig. 3(f)). Thus, the type B elements are mainly controlled by the vapor-liquid separation accompanying the input of magmatic volatiles.

Thermometric estimates

Solute geothermometers, such as those listed in Table 3, can serve as powerful tools to estimate subsurface conditions (Shan et al. 2019). The successful application of geothermometers has been discussed in the geothermal literature; their use requires five basic assumptions, as reported by Fournier (1977) and Purnomo and Pichler (2014): (1) mineral–fluid reactions are exclusively temperature dependent; (2) there is an abundance of the mineral and/or solute; (3) the system began in chemical equilibrium; (4) there has been no re-equilibration; and (5) no mixing or dilution has taken place. Different geothermometers can provide information on different water circulation environments; for example, the K/Mg geothermometer can record intermediate temperatures between the reservoir values and the spring outlet values because of its rapid re-equilibration, while the temperature

recorded by the Na/K geothermometer tends to be closer to the reservoir temperature due to the ion exchange rate (Fournier 1977; Guo and Wang 2012). Solute geothermometers mainly record the temperature in liquid-dominated systems, and when vapor-liquid separation takes place, the geothermometers mainly indicate the temperature after this process. In addition, different elements have different distribution coefficients in the vapor-liquid separation process, which also impacts the calculated results; thus, the application and evaluation of the temperatures calculated for geothermal systems should be considered carefully.

The silica geothermometers, which are known to predict temperatures closer to the outlet temperature than to the reservoir temperature (Pichler et al. 1999) and are commonly applied to hot springs ranging from 0 to 250 °C (Fournier 1977), yield predicted temperatures ranging from 100 to 200 °C in the CBS area (Table 3). Relatively low temperatures were calculated for XRQ, SBDG, CR1, and CR2; however, in the Li-Rb-Cs diagram (Fig. 7(a)), these sites had temperatures higher than 300 °C. The Si concentration is temperature dependent, and mixing, mineral precipitation during ascent, and the vapor-liquid separation process all influence Si; to avoid this inherent problem, we used the silica-enthalpy graph to calculate the enthalpy of the parent water (Fig. 8, Fournier 1977) and determined the reservoir temperature from steam tables (Keenan et al. 1969). The method predicted high temperatures ranging from 122 to 211 °C, similar to the results calculated by the Na/K geothermometer (Table 3). However, the four thermal water samples still have much lower temperatures than those indicated by the Li-Rb-Cs diagram. The Na/K geothermometer is based on the increases in the Na concentration during vapor-liquid separation and/or K-Na exchange between the fluid and the surrounding rocks (Zhao et al. 2018), while the silica geothermometers are related to the
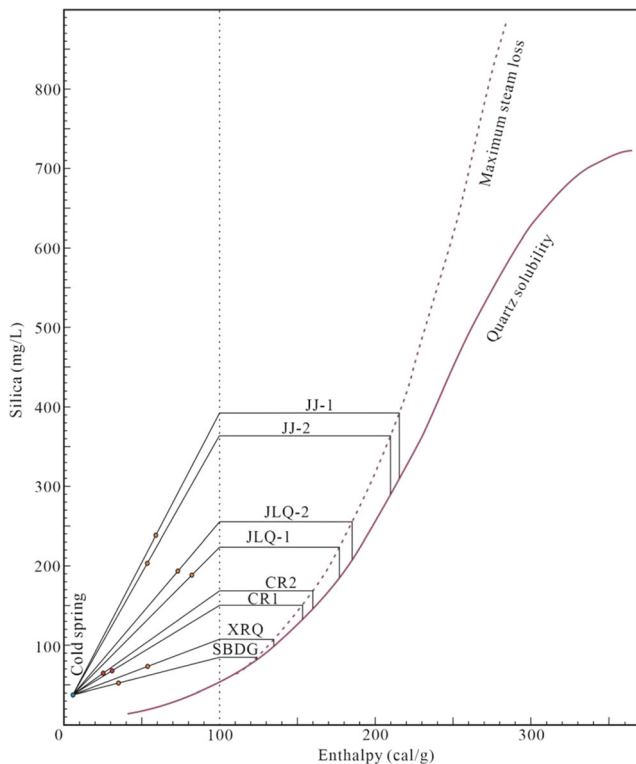
Table 3   Calculated reservoir temperatures of the Changbaishan area geothermal system

Sample	Geothermometers (°C)							
	Quartz	Quartz (steam loss)	Chalcedony	Quartz (parent)	Na/K	K/Mg	Na–K–Ca (revised)	Na/Li
JJ-1	192	178	173	211	219	91	264	269
JJ-2	181	169	160	205	205	84	329	269
JLQ-1	176	165	155	176	186	106	357	251
JLQ-2	178	166	156	182	188	106	365	254
XRQ	119	118	91	134	138	85	359	267
SBDG	104	104	74	122	152	67	299	320
CR1	117	115	88	153	114	49	127	323
CR2	114	113	85	157	111	52	118	272
Origin	Fournier 1977	Fournier 1977	Fournier 1977	Fournier 1977	Fournier 1977	Giggenbach et al. 1983	Pačes 1975	Sanjuan et al. 2014

precipitation of silicate minerals; all the thermal water samples have quartz and chalcedony SI values higher than 0 (0.42 to 0.80, 0.04 to 0.46, respectively).

The Na–K–Ca geothermometer with a pCO$_2$ correction is a useful tool for predicting the reservoir temperature of high-CO$_2$ spring waters (Pačes 1975; Fournier 1977), while the Na/Li geothermometer (Sanjuan et al. 2014; Verma and Santoyo 1997) performs well in saline water, as salinity greatly influences the results of other geothermometers (Kharaka et al. 1982; Sanjuan et al. 2014). The Na–K–Ca geothermometer

Fig. 8 Dissolved silica-enthalpy graph for determining the temperature of the parent hot-water component that mixed with cold water, thus yielding warm spring water. The graph is modified from Fournier (1977)

predicts a temperature for the low-Cl spring water of approximately 264 to 365 °C (average of 328 °C), a value that coincides with the results calculated by gas data (Shangguan et al. 1997). An increase in the Na/K ratio will decrease the calculated temperature of this geothermometer, but the effect is not as obvious as that of the Na/K geothermometer, so we regard this value as the minimum temperature of the second vapor-liquid separation temperature. The lower temperature of the two well water samples calculated by the Na–K–Ca geothermometer may be related to the extremely high Cl values (Arnórsson 1985). Thus, we use the temperature range of 272 to 323 °C (average of 297 °C) calculated by the Na/Li geothermometer as the minimum temperature of the first vapor-liquid separation.

Hydrogen and oxygen isotope consideration

The hot spring water with low Cl concentrations show δ^2H and δ^{18}O values similar to those of the meteoric water and plot between the groundwater and snow water, with some values even lower than those of meteoric water. In contrast, the δ^2H and δ^{18}O values of the high-Cl well water are much higher than those of the groundwater (Fig. 9(a)). The δ^2H and δ^{18}O values of the thermal water samples collected in and before 2016 show no obvious differences, and the region near the meteoric line of the CBS area shows precipitation recharge characteristics, as discussed by Lin et al. (1999) and Yan (2016) (Fig. 9(a)). However, the use of the mixture and fluid-rock interaction model alone cannot explain the δ^2H and δ^{18}O characteristics (e.g., Chen and Wang 2012); therefore, we introduced the vapor-liquid separation model according to the geochemical characteristics (Ingebritsen and Sorey 1988; White et al. 1971). The isotopic fractionation factors of δ^2H and δ^{18}O decrease with temperature during the vapor-liquid separation process, but δ^2H shows an inversion after 220 °C, increasing with temperature until arriving at equilibrium at approximately 370 °C (Truesdell et al. 1977).
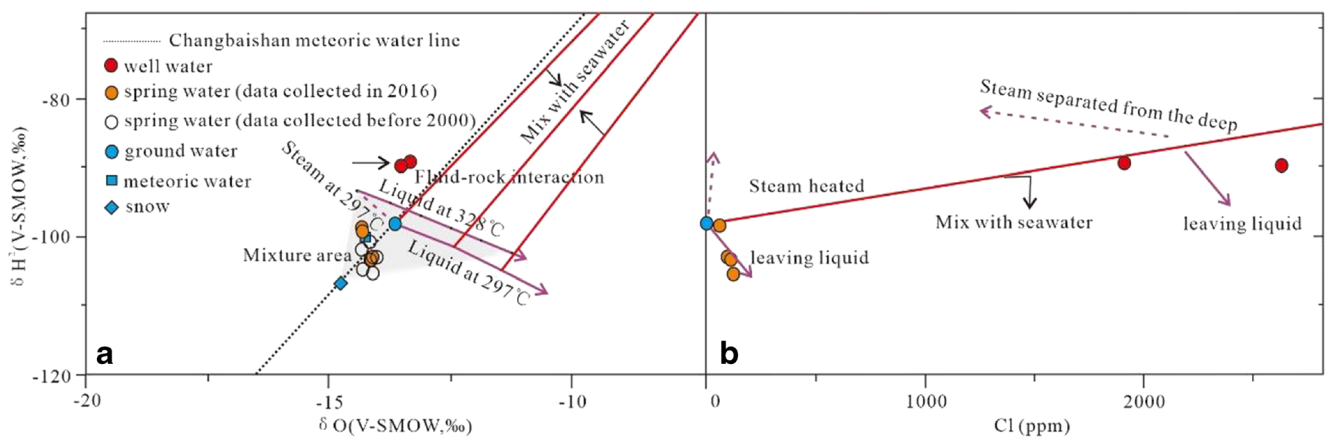
Fig. 9 δ^2H vs. $\delta^{18}O$ relations for the new and previously published data for water samples from the Changbai area (a); δ^2H vs. Cl relation (b). The δ^2H and $\delta^{18}O$ data are from Lin et al. (1999) and Yan (2016)

According to the isotopic fractionation factors of Truesdell et al. (1977) and Yi and Ni (2009), we used groundwater as the initial water, as discussed by Giggenbach and Stewart (1982), and described the isotopic variations during vapor-liquid separation at 297 °C and 328 °C (Fig. 9(a)).

The water samples from the hot springs were mainly taken from the area where the precipitation and steam-heated water mix before experiencing multiple separation processes (Fig. 9(a)). The separation process can be clearly seen in the δ^2H vs. Cl diagram (Fig. 9(b)), as chloride is a conservative component in geothermal systems and is neither soluble in steam nor leached or deposited along hot-water conduits in the upper parts of geothermal systems (Purnomo and Pichler 2014; Truesdell et al. 1977). The high-Cl water may be paleowater, as it has a δB value of approximately 35.86‰ and there are no evaporite strata in the halite precipitation stage, which implies that continental water could generate this high δB value through an intense evaporation process (Purnomo et al. 2016; Vengosh et al. 1992). If so, we hypothesize that the well water is the result of mixing between seawater and precipitation. However, even considering the vapor-liquid separation process, the plot is still above the mixing line in Fig. 9(a) but is lower in Fig. 9(b), which implies that other factors lowered the $\delta^{18}O$ value. Although the δ^2H values may also be altered, this value can be neglected (Fig. 9(b)). Generally, water samples that deviate from the meteoric water line are affected by (1) fluid-rock interactions, (2) thermochemical sulfate reduction (TSR)-H_2S, or (3) CO_2 gas (Bagheri et al. 2014; Li and Cai 2017; Tan et al. 2014). Generally, fluid-rock interactions cause the $\delta^{18}O$ value to shift to the right, while TSR-H_2S requires H_2S gas, which has not been detected in the CBS area. Thus, the ^{18}O isotope exchange between the water and CO_2 gas is the main cause of rightward shift of $\delta^{18}O$ values of the thermal water (e.g., Bagheri et al. 2014; Zhao et al. 2017), which was further supported by the small change in the $\delta^{18}O_{HCO3}$ values (32.41~34.44‰, Zhao et al. 2018).

In the continuous vapor-liquid separation process at depth, nonvolatile elements, such as Cl, Na, Li, Sr, Mg, Fe and Zn, become concentrated, while volatile constituents, such as B and CO_2, decrease in abundance. Then, the lateral migration of high-Cl water, which can exit through a fracture or well, can be detected. Hot vapor with high concentrations of volatile elements rises via buoyancy and heats the near-surface water, promoting the dissolution of rock. When the water encounters hot magmatic volatiles with high B contents, a second vapor-liquid separation can occur.

Conclusions

(1) The high Cl/B ratio and low Hg concentration implied that the fluid has experienced multiple vapor-liquid separation processes and is approaching a late-stage. Statistical analysis shows that Fe, Zn, Li, B, Sr, and Mg are mainly controlled by vapor-liquid separation in the reservoir, while the elements Cl^-, Na, and HCO_3^-, except for vapor-liquid separation, they also influenced by the input of magmatic volatiles.

(2) The Na–K–Ca geothermometer is useful to assess second vapor-liquid separation process temperature at volcanic area geothermal system. As for basin area, due to the influence of salinity, the Na/Li geothermometer will be more suitable to assess the first vapor-liquid separation process. The temperatures determined by those geothermometers are coinciding with the result of Li-Rb-Cs.

(3) Unlike liquid-dominated system model, the abnormality of hydrogen and oxygen isotopes can be explained by vapor-liquid system model. In addition, due to the large flux of CO_2, the $\delta^{18}O$ values are mainly shifted to the left of the local meteoric water line.

Declarations

Conflict of interest   The authors declare that they have no competing interests.

References

Aggarwal JK, Palmer MR, Bullen TD, Arnórsson S, Ragnarsdóttir KV (2000) The boron isotope systematics of Icelandic geothermal waters: 1. Meteoric water charged systems. Geochim Cosmochim Acta 64(4):579–585

Allen ET, Day AL (1927) Steam wells and other thermal activity at "The Geysers", vol 378. Carnegie Inst Washington Pub, Stanford, p 106

Ármannsson H, Ólafsson M (2006) Collection of geothermal fluids for chemical analysis. Report. ÍSOR-2006/016, pp 17

Ármansson H, Gíslason G, Hauksson T (1982) Magmatic gases in well fluids aid the mapping of the flow pattern in a geothermal system. Geochim Cosmochim Acta 46:167–177

Arnórsson S (1985) The use of mixing models and chemical geothermometers for estimating underground temperatures in geothermal systems. J Volcanol Geotherm Res 23:299–335

Arnórsson S, Andrésdóttir A (1995) Processes controlling the distribution of boron and chlorine in natural waters in Iceland. Geochim Cosmochim Acta 59(20):4125–4146

Arnórsson S, Stefánsson A, Bjarnason J (2007) Fluid-fluid interactions in geothermal systems. Rev Mineral Geochem 65:259–312

Bagheri R, Nadri A, Raeisi E, Eggenkamp HGM, Kazemi GA, Montaseri A (2014) Hydrochemical and isotopic ($\delta^{18}O$, $\delta^{2}H$, $^{87}Sr/^{86}Sr$, $\delta^{37}Cl$ and $\delta^{81}Br$) evidence for the origin of saline formation water in a gas reservoir. Chem Geol 384:62–75

Bernard R, Taran Y, Pennisi M, Tello E, Ramirez A (2011) Chloride and Boron behavior in fluids of Los Humeros geothermal field (Mexico): a model based on the existence of deep acid brine. Appl Geochem 26:2064–2073

Chen J, Wang Q (2012) A discussion of groundwater recharge sources in arid areas of North China. Water Resour Prot 28:1–9. (In Chinese)

Chen Y, Zhang Y, Graham D, Su S, Deng J (2007) Geochemistry of Cenozoic basalts and mantle xenoliths in Northeast China. Lithos 96(1–2):108–126

Ellis AJ, Mahon WAJ (1964) Natural hydrothermal systems and experimental hot-water/rock interactions. Geochim Cosmochim Acta 28(8):1323–1357

Ellis AJ, Mahon WAJ (1967) Natural hydrothermal systems and experimental hot water/rock interactions (Part II). Geochim Cosmochim Acta 31:519–538

Fournier RO (1977) Chemical geothermometers and mixing models for geothermal systems. Geothermics 5:41–50

Fournier RO (1989) Geochemistry and dynamics of the Yellowstone-National-Park hydrothermal system. Annu Rev Earth Planet Sci 17:13–53

Gao L, Shangguan ZG, Wei HQ, Wu CZ (2006) Recent geochemical changes of hot spring gases from Tianchi volcano area, Changbai Mountains, northeast China. Seismol Geol 28:358–366. (In Chinese)

Geological environment monitoring station of Jilin Province (2004) Report on the survey and evaluation of geothermal resources. Hua Pingchang to Jiu Zhan district in Yishu Graben, Jilin City (In Chinese)

Giggenbach WF (1988) Geothermal solute equilibria. Derivation of Na–K–Mg–Ca Geoindicators. Geochim Cosmochim Acta 52:2749–2765

Giggenbach WF (1991) Isotopic composition of geothermal water and steam discharges. Unitar (New York): Appl Geochem Geotherm Reserv Dev 253–273

Giggenbach WF (1992) Isotopic shifts in waters from geothermal and volcanic systems along convergent plate boundaries and their origin. Earth Planet Sci Lett 113:495–510

Giggenbach WF, Goguel RL (1989) Collection and analysis of geothermal and volcanic water and gas discharge. In: Department of Scientefic and Industrial Research, Chemistry Division, pp. 1989

Giggenbach WF, Stewart MK (1982) Processes controlling the isotopic composition of steam and water discharges from steam vents and steam-heated pools in geothermal areas. Geothermics 11:71–80

Giggenbach WF, Gonfiantini R, Jangi BL, Truesdell AH (1983) Isotopic and chemical composition of parbati valley geothermal discharges, North-West Himalaya, India. Geothermics 12(2–3):199–222

Guo Q, Wang Y (2012) Geochemistry of hot springs in the Tengchong hydrothermal areas, Southwestern China. J Volcanol Geotherm Res 215–216:61–73

Guo L, Ma S, Zhang Y (1996) Research on "magma chamber" of Changbai Mountain volcanoes by means of seismic tomography. CT Theor Appl 5(1):47–52. (In Chinese)

Guo Q, He T, Wu Q, Liu M (2020) Constraints of major ions and arsenic on the geological genesis of geothermal water: insight from a comparison between Xiong'an and Yangbajain, two hydrothermal systems in China. Appl Geochem 117:104589

Gurav T, Hemant KS, Chandrasekharam D (2016) Major and trace element concentrations in the geothermal springs along the west coast of Maharashtra, India. Arab J Geosci 9:44

Harun A, Hüseyin K, Halim M (2020) Hydrogeochemistry of geothermal waters in eastern Turkey: geochemical and isotopic constraints on water-rock interaction. J Volcanol Geotherm Res 390(15):104708

Heinrich C (2007) Fluid-fluid interactions in magmatic hydrothermal ore formation. In: Liebscher A, Heinrich CA (eds), Rev Min Geochem 65:363–387

Henley RW, Hughes GO (2000) Underground fumaroles: "Excess Heat" effects in vein formation. Econ Geol 95(3):453–466

Heřmanská M, Kleine BI, Stefánsson A (2020) Geochemical constraints on supercritical fluids in geothermal systems. J Volcanol Geotherm Res 394:206824

Huang JJ, Xu ZH, Xun NR, Niu JP (2020) Evaluation of geothermal resource potential of Xidaogou geothermal resources in Changbai County, Basalt overburden area of Changbai Mountain, Jilin Province. Sci Technol Innov 34:157–158 (In Chinese)

Ingebritsen SE, Sorey ML (1988) Vapor-dominated zones within hydrothermal systems: evolution and natural state. J Geophys Res 93(B11):13635–13655

Janik CJ, Mclaren MK (2010) Seismicity and fluid geochemistry at Lassen Volcanic National Park, California: evidence of two circulation cells in the hydrothermal system. J Volcanol Geotherm Res 189:257–277

Jiang Q, Chen J (2015) Analysis on water balance of deep cycle groundwater supplying Tianchi Lake of Changbai Mountain. Water Resour Prot 31(5):7–13. (In Chinese)

Kaasalainen H, Stefánsson A (2012) The chemistry of trace elements in surface geothermal waters and steam, Iceland. Chem Geol 330–331:60–85

Kaasalainen H, Stefánsson A, Giroud N, Arnórsson S (2015) The geochemistry of trace elements in geothermal fluids, Iceland. Appl Geochem 62:207–223

Karimi S, Mohammadi Z, Samani N (2017) Geothermometry and circulation depth of groundwater in Semnan thermal springs, Northern Iran. Environ Earth Sci 76:659

Keenan JH, Keyes FG, Hill PG, Moore JG (1969) Steam Tables. Wiley, New York

Kharaka YK, Lico MS, Law LM (1982) Chemical geothermometers applied to formation waters, Gulf of Mexico and California Basins (abstract). Am Assoc Pet Geol Bull 66:588

Leeman WP, Tonarini S, Pennisi M, Ferrara G (2005) Boron isotopic variations in fumarolic condensates and thermal waters from Vulcano Island, Italy: implications for evolution of volcanic fluids. Geochim Cosmochim Acta 69:143–163

Li H, Cai C (2017) Origin and evolution of formation water from the Ordovician carbonate reservoir in the Tazhong area, Tarim Basin, NW China. J Pet Sci Eng 148:103–114

Lin Y, Gao Q, Yu Q (1999) A study of chemical characteristics of geothermal fluid in Tianchi Volcanic Region, Changbai Mountains. Geol Rev 45(Sup):241–247 (In Chinese)

Liu R, Chou S, Cai L, Wei H, Yang Q, Xi Z, Bo G, Zhong J (1997) The date of last large eruption of Changbaishan - Tianchi volcano and its significance. Sci China Ser D Earth Sci 27(5):437–441 (In Chinese)

Liu J, Chen S, Guo W, Sun C, Zhang M, Guo F (2015) Research advances in the Mt. Changbai Volcano. Bull Mineral Petrol Geochem 34(4):710–723

Negri A, Daniele L, Aravena D, Muñoz M, Delgado A, Morata D (2018) Decoding fjord water contribution and geochemical processes in the Aysen thermal springs (Southern Patagonia, Chile). J Geochem Explor 185:1–13

Nuccio PM, Paonita A, Sortino F (1999) Geochemical modeling of mixing between magmatic and hydrothermal gases: the case of Vulcano Island, Italy. Earth Planet Sc Let 167:321–333

Pačes T (1975) A systematic deviation from Na-K-Ca geothermometer below 75°C and above $10^{-4} \sim$ atm P_{CO_2}. Geochim Cosmochim Acta 39:541–544

Parkhurst DL, Appelo CAJ (1999) User's guide to PHREEQC (Version 2)—a computer program for speciation, batch-reaction, onedimensional transport, and inverse geochemical calculations. Water Resources Investigations Report (United States Geological Survey) 99–4259

Pichler T, Veizer J, Hall GEM (1999) The chemical composition of shallow-water hydrothermal fluids in Tutum Bay, Ambitle island, Papua New Guinea and their effect on ambient seawater. Mar Chem 64:229–252

Purnomo BJ, Pichler T (2014) Geothermal systems on the island of Java, Indonesia. J Volcanol Geotherm Res 285:47–59

Purnomo BJ, Pichler T, You CF (2016) Boron isotope variations in geothermal systems on Java, Indonesia. J Volcanol Geotherm Res 311:1–8

Qiu G, Fei F, Fang H, Du B, Zhang X, Zhang P, Yuan Y, He M, Bai D (2014) Analysis of magma chamber at the Tianchi volcano area in Changbaishan mountain. Chin J Geophys 57(10):3466–3477 (In Chinese)

Rahayudin Y, Kashiwaya K, Tada Y, Iskandar I, Koike K, Atmaja RW, Herdianita NR (2020) On the origin and evolution of geothermal fluids in the Patuha Geothermal Field, Indonesia based on geochemical and stable isotope data. Appl Geochem 114:104530

Sanjuan B, Romain M, Asmundsson R, Michel B, Giroud N (2014) Use of two new Na/Li geothermometric relationships for geothermal fluids in volcanic environments. Chem Geol 389:60–81

Scot S, Gunnarsson I, Arnórsson S, Andrésdóttir A (2014) Gas chemistry, boiling and phase segregation in a geothermal system, Hellisheidi, Iceland. Geochim Cosmochim Acta 124:170–189

Scott S, Driesner T, Weis P (2017) Boiling and condensation of saline geothermal fluids above magmatic intrusions. Geophys Res Lett 44:1696–1705

Shan X, Cai Z, Hao G, Zhou X, Zhao R (2019) Estimation of thermal storage temperature of geothermal system in Changbai Mountain by geothermometers. J Jilin Univ (Earth Sci Ed) 49(3):662–672 (In Chinese)

Shangguan Z, Sun L, Sun F, Gao S (1996) Deep-seated fluid components and stable isotopic compositions in Tianchi volcanic area, Changbaishan Mountains. Sci Geogr Sin 31(1):54–64 (In Chinese)

Shangguan Z, Zheng Y, Dong J (1997) Material sources of escaped gases from Tianchi volcanic geothermal area, Changbai Mountains. Sci China Ser D Earth Sci 40(4):390–397

Shi L, Chen X, Yang Q, Wei H, Lin C (2005) Petrochemistry of pumices of various colors produced by the eruption of Changbaishan Tianchi volcano at 1000 years ago. Seismol Geol 27(1):73–82

Stefánsson A, Hilton DR, Sveinbjörnsdóttir ÁE, Torssander P, Heinemeier J, Barnes JD, Ono S, Halldórsson SA, Fiebig J, Arnórsson S (2017) Isotope systematics of Icelandic thermal fluids. J Volcanol Geotherm Res 337:146–164

Tan H, Zhang Y, Zhang W, Kong N, Zhang Q, Huang J (2014) Understanding the circulation of geothermal waters in the Tibetan Plateau using oxygen and hydrogen stable isotopes. Appl Geochem 51:23–32

Truesdell AH, Nathenson M, Rye RO (1977) The effects of subsurface boiling and dilution on the isotopic composition of Yellowstone thermal waters. J geophys Res 82:3694–3704

Truesdell AH, Haizlip JR, Armannsson H, D'Amore F (1989) Origin and transport of chloride in superheated geothermal steam. Geothermics 18:295–304

Valentio GM, Stanzione D (2003) Source processes of the thermal waters from the Phlegraean Fields (Naples, Italy) by means of the study of selected minor and trace elements distribution. Chem Geol 194:245–274

Vengosh A, Starinsky A, Kolodny Y, Chivas AR (1991) Boron isotope geochemistry as a tracer for the evolution of brines and associated hot springs from the Dead Sea, Israel. Geochim Cosmochim Acta 55:1689–1695

Vengosh A, Starinsky A, Kolodny Y, Chivas AR, Raab M (1992) Boron isotope variations during fractional evaporation of sea water: new constraints on the marine vs. nonmarine debate. Geology 20:799–802

Verma SP, Santoyo E (1997) New improved equations for Na/K, Na/Li and SiO_2 geothermometers by outlier detection and rejection. J Volcanol Geotherm Res 79:9–23

Wang Y, Li C, Wei H, Shan X (2003) Late Pliocene–recent tectonic setting for the Tianchi volcanic zone, Changbai Mountains, northeast China. J Asian Earth Sci 21(10):1159–1170

Wei H, Liu G, Gill J (2013) Review of eruptive activity at Tianchi volcano, Changbaishan, northeast China: implications for possible future eruptions. Bull Volcanol 75:706

White DE (1957) Thermal waters of volcanic origin. Geol Soc Am Bull 68:1637–1658

White DE, Muffler LJ, Truesdell AH (1971) Vapor-dominated hydrothermal systems compared with hot-water system. Econ Geol 66:75–97

Wragea J, Tardania D, Reicha M, Danielea L, Arancibiab G, Cembranob J, Sánchez-Alfaroa P, Morataa D, Pérez-Morenoa R (2017)

Geochemistry of thermal waters in the Southern Volcanic Zone, Chile—implications for structural controls on geothermal fluid composition. Chem Geol 466:545–561

Xu D, Zheng X, Xu X (1993) Holocene volcanic activities and their features in tianchi area, Changbaishan mountains. Quaternary Sci 1:85–94. (In Chinese)

Yan B (2016) Study on the formation mechanism of geothermal water resources in Changbai Mountain basalt area. Jilin University of Environment and Resources (In Chinese)

Yan B, Xiao C, Liang X, Wu S (2016) Hydrogeochemical tracing of mineral water in Jingyu County, Northeast China. Environ Geochem Health 38:291–307

Yi G, Ni S (2009) Isotope geochemistry. Geology Publishing House, Bejing (in Chinese)

Yi J, Wang P, Gao Y, Yao R, Zhao R, Chen C (2016) Vesicle distribution in basalt lava flow units in the Mesozoic rift basins of northeast China and its application in gas reservoir prediction. Can J Earth Sci 53:59–70

Yu GM, Zhang XN, Wang CS (1990) Geological interpretation on the results of cluster analysis of trace elements from argillaceous rocks in the Jurassic, Cretaceous and Tertiary strata in Xizang. Lithof Paleogeogr 5(5):1–7. (In Chinese)

Zhang X, Li G (2006) The geologic and geochemical characteristics of the Changbai Mountain geothermal field. Jilin Geo 25(1): 25–30. (In Chinese)

Zhang M, Guo Z, Sano Y, Cheng Z, Zhang L (2015) Stagnant subducted Pacific slab-derived CO_2 emissions: insights into magma degassing at Changbaishan volcano, NE China. J Asian Earth Sci 106:49–63

Zhao DP, Tian Y, Lei JS, Liu L, Zheng SH (2009) Seismic image and origin of the Changbai intraplate volcano in East Asia: role of big mantle wedge above the stagnant Pacific slab. Phys Earth Planet Inter 173:197–206

Zhao R, Shan X, Yi J, Du X, Liang Y, Zhang Y (2017) Geochemistry of HCO_3-Na thermal water from the Gudian slope: Insights into fluid origin, formation mechanism and circulation in the Yitong Basin, Northeast. Appl Geochem 91:185–196

Zhao R, Shan X, Yi J, Liang Y, Li C, Qiu C (2018) Understanding fluid behavior through ion and isotope data from the Yitong Basin, Northeast China. Can J Earth Sci 55:308–320

Zhao R, Shan X, Wu C, Yi J, Hao G, Wang P (2019) Formation and evolution of the Changbaishan volcanic geothermal system in a convergent plate boundary back-arc region constrained by boron isotope and gas data. J Hydrol 569: 188–202

Zhu Y, She Z, Fu D, Huang X (1981) The hydrochemistry of Tian-chi (crater) lake of the Chang-bai Mountains. Sci Geogr Sin 1(1):59–65. (In Chinese)